(K0.5Bi0.5)ZrO3 (KBZ) lead-free perovskite compound: Structural study and physical properties

Jerome Lelievre, Michaël Josse, Pascal Marchet

$(K_{0.5}Bi_{0.5})ZrO_3$ (KBZ) lead-free perovskite compound: structural study and physical properties

Jerome Lelievre[1], M. Josse[2] and Pascal Marchet[1,]*

1. Univ. Limoges, CNRS, IRCER, UMR 7315, F-87000 Limoges, France

2. CNRS, Univ. Bordeaux, ICMCB, UMR 5026, F-33600 Pessac, France

* Corresponding Author.

E-mail address: pascal.marchet@unilim.fr

KEYWORDS

Lead-free perovskite; X-Ray diffraction; Neutron Diffraction, crystal structure; electrostriction

ABSTRACT

The structural study of $(K_{0.5}Bi_{0.5})ZrO_3$ compound (KBZ) evidenced a cubic ABO_3 perovskite structure (space group: No 221 Pm3m, lattice parameter: a = 0.4157 nm). Above room temperature, the lattice parameter increases linearly, with linear expansion coefficient α = 6.4 x 10^{-6} K^{-1}. No phase transition or decomposition occurs up to 1273 K (1000°C). Below room temperature, small anomalies in Differential Scanning Calorimetry (DSC) and dielectric losses (tan(δ)) remain structurally unexplained and will need further investigation. Furthermore, KBZ

appears as difficult to sinter. Although the A-site of the ABO_3 perovskite lattice is occupied by two ions of different valences (K^+/Bi^{3+}, mixed occupancy), we did not detect relaxor behaviour in KBZ dielectric properties. However, electrostriction was observed at room temperature. This property, combined to the limited thermal evolution of the relative permittivity indicate that KBZ may be an interesting material, provided that the sintering can be improved.

Introduction

Currently, electronic devices are omnipresent in our everyday life, which make piezoelectric and ferroelectric materials an important and discreet part of our life. These materials are used everywhere: cars, mobile phones, electronic memory systems... Nowadays, $Pb(Zr_{1-x}Ti_x)O_3$ (PZT) are the most used compounds due to their high electromechanical properties, low-cost, and the possibility to use them in a large range of applications [1]. However, lead is a harmful element associated to health and environmental issues. Therefore, the use of lead is now restricted by European regulations (RoHS, WEEE) [2,3]: lead is still tolerated in electronic devices but has yet to be replaced.

Consequently, a huge scientific effort started about 20 years ago in order to find lead-free compounds suitable to substitute PZT. Nowadays, most of the lead-free materials considered have a ABO_3 perovskite structure: (i) $BaTiO_3$-based materials, (ii) niobates such as $(K,Na)NbO_3$ (KNN), (iii) alkaline titanates like $(Na_{0.5}Bi_{0.5})TiO_3$ (NBT) or $(K_{0.5}Bi_{0.5})TiO_3$ (KBT) and (iv) solid solution of these materials such as $(1-x)(Na_{0.5}Bi_{0.5})TiO_3 - xBaTiO_3$ (NBT-BT) [4–16].

Among these materials, NBT is promising because of its ferroelectric – piezoelectric properties (d_{33} = 80 pC/N, Pr = 38 μC/cm²) [17,18]. NBT was first reported by Smolenskii in the 1960s, proving the possibility to substitute Pb^{2+} by (Na^+/Bi^{3+}) pseudo-ion in the A-site of the ABO_3

perovskite lattice, confirmed for (K^+/Bi^{3+}) by the discovery of KBT [19]. Thus, it was tempting to try substitutions in the B-site, like for the $PbTiO_3$ or $BaTiO_3$ perovskite compounds, for which the existence of $PbZrO_3$ and $BaZrO_3$ compounds proves this possibility.

Smolenskii first considered this substitution, suggesting the existence of the $(Na_{0.5}Bi_{0.5})ZrO_3$ (NBZ) and $(K_{0.5}Bi_{0.5})ZrO_3$ (KBZ) compounds [20]. Unfortunately, he reported only dielectric measurements, without X-ray diffraction (XRD) patterns. In 1995, a study devoted to the dielectric properties of the NBT-NBZ-KBT-KBZ system reported the possible occurrence of NBZ and KBZ compounds, (without XRD pattern) [21]. In 2007, NBZ was evidenced, XRD pattern reported [22,23] and the NBZ compound studied [21–28]. In contrast, there are very few reports devoted to KBZ. Indeed, most of the articles focus on solid solutions with other compounds, such as KBT or KNN [21,29–34].

According to the only available XRD data [35], KBZ should be cubic, without any piezoelectric or ferroelectric properties (Pm3m centrosymmetric space group). However, these XRD data are based upon unpublished results. Currently, there is no report on structural study of KBZ. Therefore, the cubic structure and space group shall be confirmed. In addition, KBZ presents a mixed occupancy of the A-site. As for NBT or PMN [36,37], this mixed occupancy can induce a relaxor behaviour and perhaps electrostrictive properties. To our knowledge, such phenomenon was never studied for KBZ. Therefore, the aims of the present work are: (i) to determine the structure of KBZ compound, (ii) to study its electrical properties (relaxor behaviour, electrostriction) and (iii) to search for possible phase transitions above and below room temperature

1. Materials and Methods

The KBZ compound was synthesized in alumina crucible, using K_2CO_3 (Aldrich, 99+%), Bi_2O_3 (Puretech, 99.975%) and ZrO_2 (Alfa Aesar, 99.978%) in stoichiometric amounts. The calcination

was carried out at 800°C for 4h (5°C.min^{-1} ramp). After synthesis, X-Ray diffraction (XRD, θ/2θ diffractometer, Bruker D8, Cu Kα1) evidenced for a perovskite compound (similar to PDF 00-067-0245). As previously reported, unreacted ZrO_2 was also observed (around 3.4 mol%) [28,29,31]. A larger batch prepared for neutron diffraction experiments (20g) unfortunately revealed a larger amount of ZrO_2 (16.9 mol%). The weight losses (volatilization of potassium and bismuth) were also checked and are lowers than 0.5 %. The crystallographic study has been led both by neutron powder diffraction (NPD, Leon Brillouin Laboratory, 3T2 diffractometer, Saclay, France) and XRD. Powder XRD data were collected at 20°C (12 hours, step size: 0.0118406°, 2θ = 20-120°, Cu Kα1, λ=1.5406 Å). Structural resolution was performed by the Rietveld method (Jana 2006 software [38]). Dilatometry measurements were performed before sintering (25-1000°C, Setaram TMA Setsys Evolution 1600). A plasticizer and a binder (polyethylene glycol and polyvinyl alcohol) were added to the powder before shaping, which was performed by uniaxial pressing (250 MPa, 10 mm diameter). Sintering was carried out at 900°C for 4h (5°C.min^{-1} ramp). Dielectric measurements were performed between 80K and 450K using an impedance analyser (Agilent 4194A). In order to search for phase transitions, thermal analysis was performed on powders (100-350K, DSC Q1000, TA Instruments; 300-1273K, DTA/TG Setaram Labsys Evo 1600). High temperature X-Ray diffraction (HT-XRD) was also used (300-1273K) in order to study high temperature behaviour.

2. Results

2.1. Structural study at room temperature

2.1.1. X-ray powder diffraction

After synthesis and as noticed hereabove, XRD pattern evidenced the occurrence of unreacted ZrO_2 (3.4 mol%), in addition to the KBZ perovskite compound. Considering the reported diffraction pattern (PDF 00-067-0245) and the absence of extra peaks nor splitting of perovskite

peaks, KBZ should be cubic. The calculation of the Goldschmidt tolerance factor "t" supports this assumption. Its value is defined as: $= \frac{(R_A+R_O)}{\sqrt{2}.(R_B+R_O)}$, where R_A, R_B and R_O are respectively the ionic radii of A ion (coordination number CN = 12), B ion (CN = 6) and oxygen ion [39–41]. This factor is only a guide for the prediction of stability and distortions of perovskites structures, considered as stable for $0.88 \leq t \leq 1.05$. The cubic prototype structure (Pm3m) corresponds to $t = 1$. For $t < 1$, the structure is distorted and presents octahedra tilting, described by Glazer with 23 possible tilt systems [42,43], later reduced to 15 possible systems by Howard and Stokes [44]. For $t > 1$, the B ion is too small for the octahedral site. The cation move out of the octahedra center in order to reduce the B-O bond length and decrease its coordination number. This case generally leads to polar -ferroelectric structure (like $BaTiO_3$ or $PbTiO_3$).

For KBZ, $t = 0.97$ ($t = 1.04$ for the polar ferroelectric tetragonal titanate compound KBT). Thus, KBZ is very close to cubic. The attempts to refine the structure using other symmetries associated to low distortion (orthorhombic, rhombohedral or tetragonal) led to unrealistic results. Therefore, the most probable solution is cubic, as reported for KBT-KBZ- solid solution [29].

The atomic positions were first defined as in the prototype cubic perovskite structure, with (K^+/Bi^{3+}) at the origin of the cell. The ratio K/Bi had also been refined and showed a small difference with the initial composition. The agreement factors for the refinement are acceptable, even if R_p and R_{wp} may be a bit high (Table 1 – fig. 1). However, the atomic displacement parameters (ADP) are quite high for (K^+/Bi^{3+}) and oxygen ion.

Table 1: Refined crystallographic parameters for KBZ obtained by XRD, with final formula $(K_{0.48}Bi_{0.52})ZrO_3$

Atoms	Site	Occupancy	x	y	z	U_{iso}
K	1a	0.48	0	0	0	0.1445
Bi	1a	0.52	0	0	0	0.1445
Zr	1b	1	0.5	0.5	0.5	0.0033
O	12h	1	0.5	0.5	0	0.0296
Space group: $Pm\bar{3}m$				K/Bi Ratio: 0.48 / 0.52		
GoF = 2.41		R_p = 6.19%		R_{wp} = 8.68%		
Second phase: ZrO_2 3.4mol%						

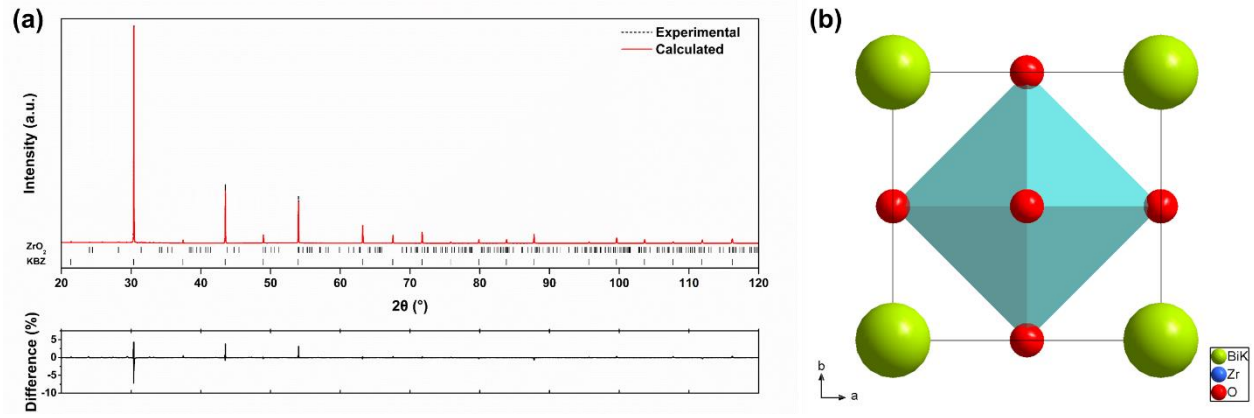

Figure 1: (a) Room temperature XRD pattern of KBZ powder and results of the Rietveld crystallographic refinement, taking into account ZrO_2 as a second phase (b) representation of the obtained KBZ structure along the [001] direction (color online)

For PMN, structural studies revealed a long-range mean cubic structure (Pm3m). The global Mg:Nb chemical order (B-site) is 1/3:2/3, but locally deviates from this ratio, inducing local polar clusters responsible for the PMN relaxor properties. Therefore, PMN mean structure was described either by an ordered structure or by a local disorder involving the A-site or the B-site, or even both sites simultaneously [45,46]. For KBZ, we attempted to reduce the ADP for (K^+/Bi^{3+}) pseudo-ion

by splitting of the "1a" (0 0 0) site, but this did not lead to consistent improvements. This result, with high ADP factors, has finally the same order of magnitude as the values reported for equivalent compounds such as KBT and NBT [47,48]. Therefore, these high values could be due to the mixed occupancy of the A site. Indeed, on one hand, Bi^{3+} ion is non-spherical (stereochemical activity of the $6s^2$ lone electron pair), on the other hand K^+ ion is spherical and thus should occupy the center of the A-site. These considerations will need further study of the local order.

2.1.2. neutron powder diffraction

The high isotropic ADP parameter on the oxygen site could be due to a structural disorder, as observed for PMN. This possibility has been studied in a second step by Neutron Diffraction, which allow a better resolution on oxygen ions.

The first refinement had been carried out with atoms positioned as in the prototype cubic perovskite, presented in the XRD pattern (Fig. 1). The agreement factors obtained are a bit high (GoF = 4,60, Rp = 3,55%, Rwp = 5,59%) but acceptable, indicating that the structural model can be improved. Attempts to reduce the ADP factors for the (K^+/Bi^{3+}) ion (U_i = 0.0890), by modifying their positions, were unsuccessful. Then, we tried different possible positions for the oxygen ions, that also present high ADP factors (U_i = 0.0312). Most of them led to lower quality results or diverging refinement. However, splitting the 3c oxygen site $(0,\frac{1}{2},\frac{1}{2})$ on the 12h site $(0,\frac{1}{2},x)$ improved subsequently the quality of the refinement (GoF= 2,87, Rp= 2,65%, Rwp= 3,49%) and decreased the ADP factor of oxygen ions to more satisfying values. (Table 2) The observed calculated and differences curves of this final refinement are represented in figure 2.

Table 2: Refined crystallographic parameters for KBZ obtained by neutron diffraction (NPD)

Atoms	Site	Occupancy	x	y	z	U_{iso}
K	1a	0.51	0	0	0	0.0864
Bi	1a	0.49	0	0	0	0.0864
Zr	1b	1	0.5	0.5	0.5	0.0023
O	12h	1	0.567	0.5	0	0.0006
Space group: $Pm\bar{3}m$					K/Bi ratio: 0.51/0/49	
GOF: 2.87		Rp = 2.65%			Rwp = 3.49%	
Second phase: ZrO_2 = 16.9mol%						

This result indicates, at least locally, a departure from the prototype cubic structure. This could be the sign of precessing octahedral chains, as observed for example in the $RbAl_2Tb_4F_{22}$ compound [49]. Such a structural feature could be induced by mismatching of K/Bi ions with respect to the perovskite octahedral framework, resulting in such precessing chains that would not appear "tilted" (on average, they are straight) but that could stabilize in a periodic or aperiodic modulated structure.

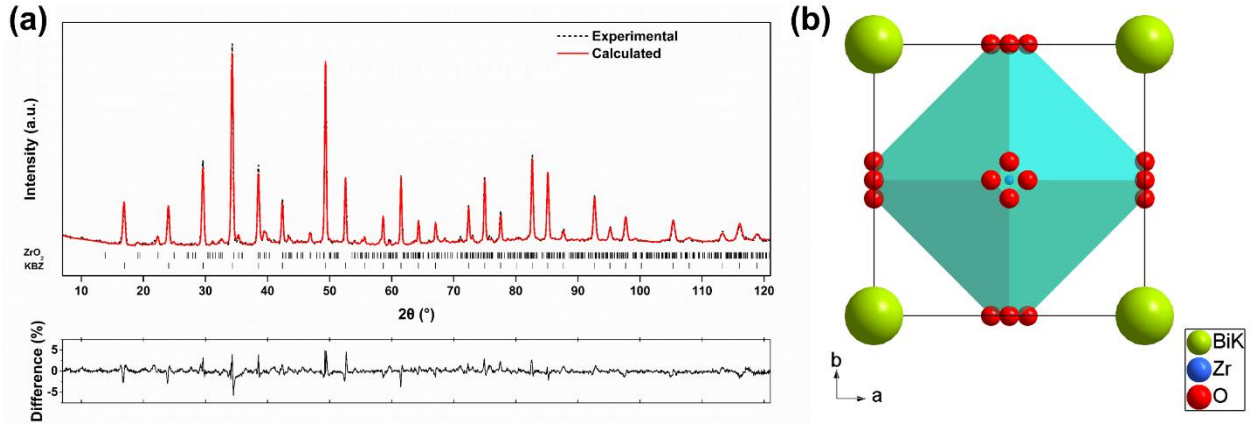

Figure 2: (a) Room temperature neutron diffraction pattern of KBZ powder obtained by neutron diffraction and the results of the Rietveld crystallographic refinement, taking into account ZrO_2 as a second phase (b) representation of the obtained KBZ structure along the [001] direction (color online)

Finally, the structure of KBZ is cubic (Pm3m, $a_p = 4.158$Å), described as a shared corner network of ZrO_6 octahedra, without octahedra rotation (Glazer notation is $a^0a^0a^0$) The K^+/Bi^{3+} pseudo-ion occupies the cuboctahedral A-site between 12 ZrO_6 octahedra. The distance between A-ion and oxygen-ion is 2.94 Å, in good agreement with the sum of the ionic radii of K^+/Bi^{3+} pseudo-ion and oxygen ion (1.51 + 1.40 = 2.91 Å). The Zr-O bond length (2.079 Å) is only slightly lower than the sum of the ionic radius of Zr^{4+} and oxygen ion (0.72 + 1.40 = 2.12 Å).

2.2. Electrical properties

As the refined structure is centrosymmetric, KBZ is not expected to have piezoelectric nor ferroelectric properties [50]. Furthermore, since the room temperature structure is cubic, phase transitions can possibly occur below room temperature. In addition and because of the mixed occupancy of the A-site by the (K^+/Bi^{3+}) pseudo-ion, KBZ can also exhibit relaxor and electrostrictive properties. Thus, the electrical properties were studied as a function of temperature (ε_r, tan(δ)), as well as the thermal behaviour (DSC and DTA/TG).

Unfortunately, the KBZ compound appears as difficult to sinter. Dilatometry measurements performed up to 1273 K (1000°C) evidenced that there is nearly no shrinkage for this temperature range (0.7% - Fig. S1). Increasing the sintering temperature led to an important weight loss (volatility of K/Bi ions). Sintering using other technics (Spark Plasma Sintering, reactive sintering) did not improve the final density. However, XRD measurements on the final pellets showed that there was no decomposition of the perovskite compound during the sintering process up to 1273K (1000°C). The only second phase observed remains ZrO_2. Therefore, we performed electrical measurement for sintered samples with relative density only between 80% and 90%.

2.2.1. Electrostriction

Concerning the room temperature properties, measurements of the mechanical displacement induced by electrical field were performed, in order to check for electrostriction. Current density

was also measured in order to confirm the assumption of high conductivity due to a lack of densification (same pellet for both measurements). The J = f(V) curve (fig. 3) evidences that DC conduction appears quickly (around 1000 V/mm), confirming poor insulating properties related to low densification of the sample. Furthermore, mechanical displacement measurements (fig. 3) revealed electrostriction (parabolic law). The evaluation of the electrostrictive coefficient by fitting of the strain curve led to $M_{33} = 4.5 \pm 0.2 \times 10^{-20}$ $m^2.V^{-1}$, four order of magnitude smaller than for PMN [51]. However, due to the important DC leakages it was not possible to determine totally the slope of the curve. Therefore, this phenomenon will need further study, notably by improvement of the density of the samples.

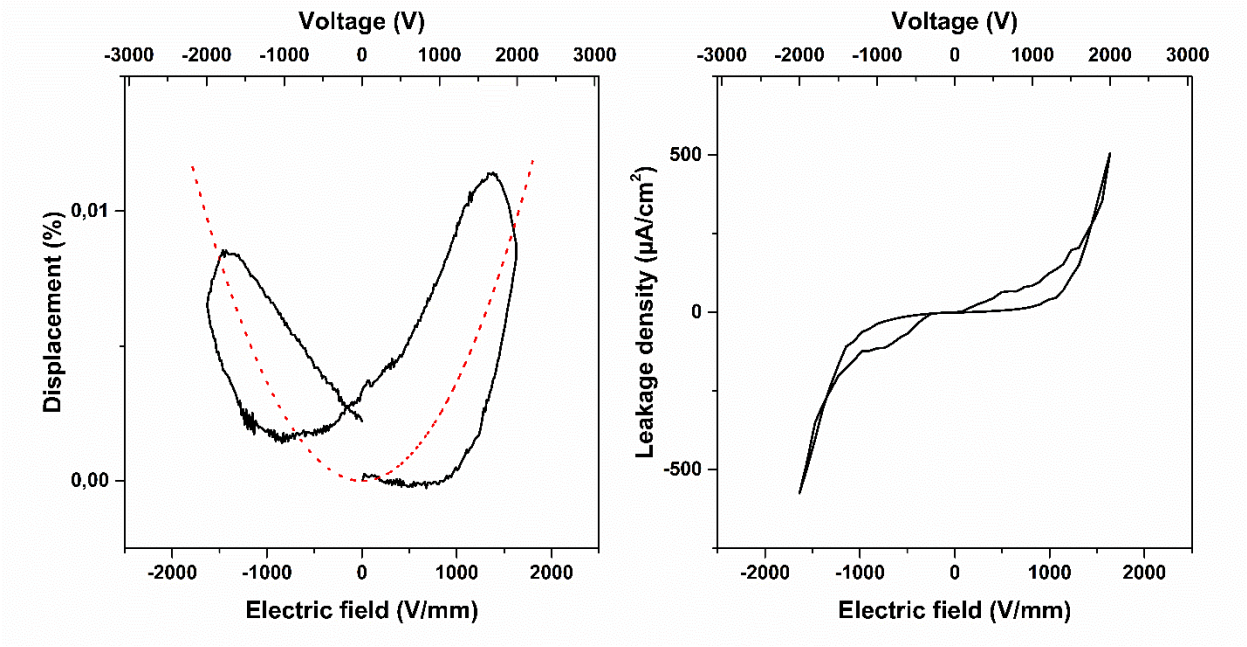

Figure 3: representations of (left) displacement measurement and (right) leakage current density j = f(V) as a function of voltage and electric field for KBZ pellet (color online)

2.2.2. Dielectric properties as a function of temperature

In order to check for relaxor behaviour and possible phase transitions, the relative permittivity ε_r and dielectric losses tan(δ) were investigated between 80K and 450K (100Hz to 1MHz, fig. 4).

The behaviour was not studied at higher temperature due to poor densification. Indeed, the tan(δ) values increase quickly above 300-350K, indicating conduction, thus confirming room temperature J = f(V) measurements. Around 350-400K, a "hump" is observed in ε_r. Considering tan(δ) values (more than 10% for lowest frequencies), this phenomenon is likely associated to an extrinsic source (defects, space charges, interfacial phenomena…).

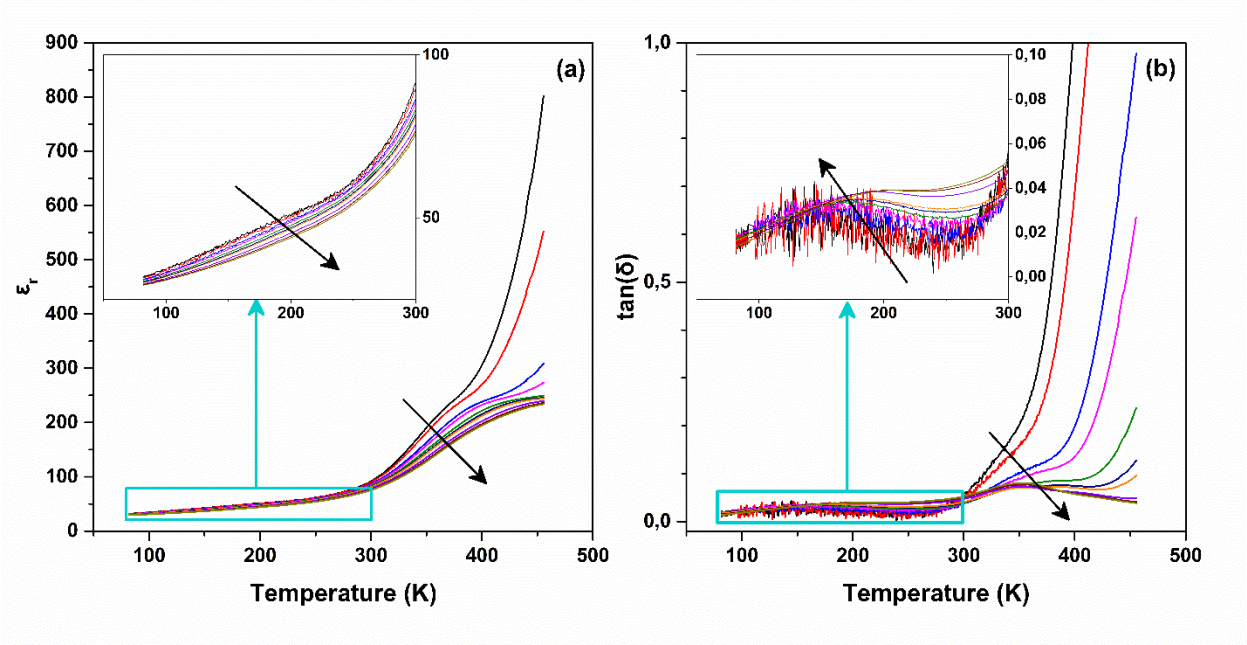

Figure 4: Evolution of (a) the relative permittivity ε_r and (b) the dielectric losses tan(δ) as a function of temperature for different frequencies (524.8Hz, 1kHz, 5.25kHz, 10kHz, 33.1kHz, 69.2kHz, 100kHz, 331.1kHz, 691.8kHz and 1MHz; the black arrows indicate increasing frequencies) (color online)

2.3. Thermal evolution and possible phase transition below room temperature

The low temperature part of the permittivity curves (100 – 300K, Fig. 4) presents a nearly linear increase of ε_r. The only anomaly (between 100K and 250K) is a broad dispersion of tan(δ), of very small amplitude, which is frequency dependent. Simultaneously, there is not perceptible peak of ε_r, and only a small dispersion of permittivity as a function of frequency. Thus, this anomaly may

not be associated to a relaxor behaviour and could be the signature of a minor structural relaxation (BO_6 polyhedra tilting?).

Therefore, DSC measurement was carried out in this temperatures range, in order to check for the possibility of a phase transition (Fig. 5). However, we did not detect any thermal phenomenon indicating a phase transition between 100K and 250K. Nevertheless, a small discontinuity of the baseline was detected (280-290K for cooling run and 250-260K for heating run). This small anomaly may not be directly connected to that observed during dielectric measurements, although it appears near the temperature at which the tan(δ) dispersion closes. Further structural investigation below room temperature will be necessary in order to identify the origin of this anomaly.

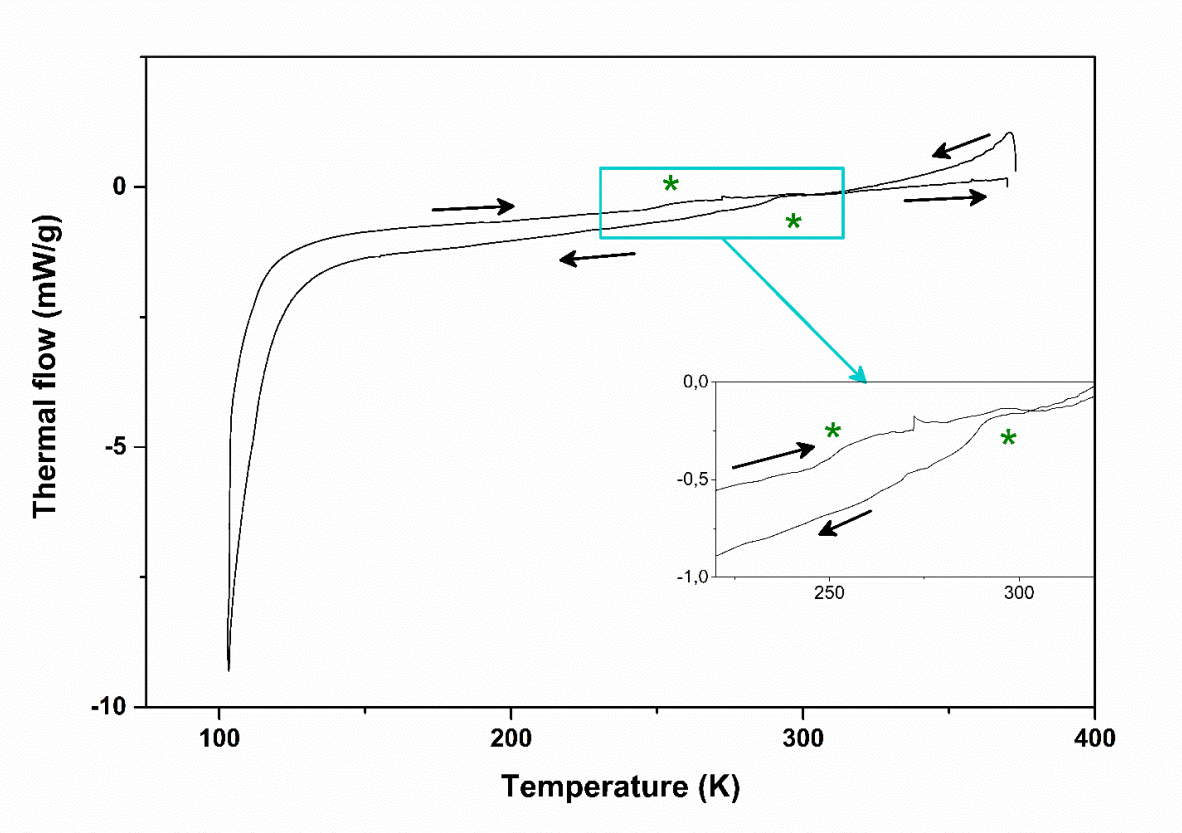

Figure 5: DSC of KBZ powder between 100K and 350K (the arrows indicate heating and cooling run respectively). The green symbol (*) point out an anomaly observed during heating (250-260K) and cooling (280-290K) runs (color online)

2.3. Thermal evolution above room temperature

In order to search for phase transition above room temperature (or decomposition), HT-XRD was also performed (Fig. S2). Logically, there is no evidence of a symmetry change with temperature (room temperature structure is prototype structure). The thermal evolution of the lattice parameter is linear (fig. 6), in agreement with the absence of phase transition. The corresponding expansion coefficient is $\alpha \approx 6.4.10^{-6}$ K^{-1}, similar to other perovskite compounds [52]. The study of possible structural changes above room temperature has also been led by DTA/TG (Fig. 7), showing two thermal phenomena. The first one (450K) is irreversible and associated to a small weight loss. Thus, it could be due to water desorption. The second one (860-885K) is reversible, of small amplitude, and is probably correlated to the transient small extra peak observed by HT-XRD. Since these XRD small peaks are not connected to KBZ, this thermal event is probably associated to unreacted ZrO_2 secondary phase. However, the weight losses are very limited (0.25 – 0.3%), confirming that KBZ compound is thermally stable up to up to 1273K (1000°C), as observed during sintering study.

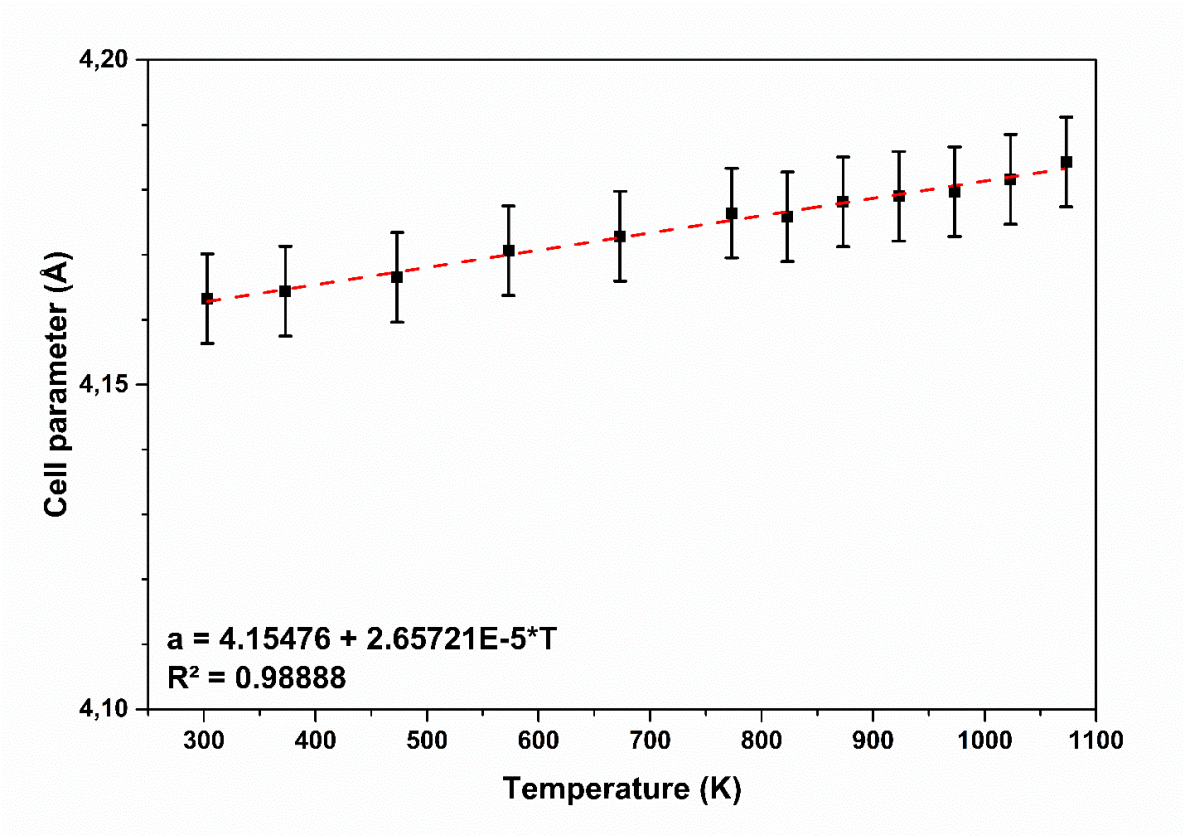

Figure 6: Evolution of the cell parameter of KBZ with temperature (from room temperature to 800°C), obtained by refinement of the HTXRD patterns (color online)

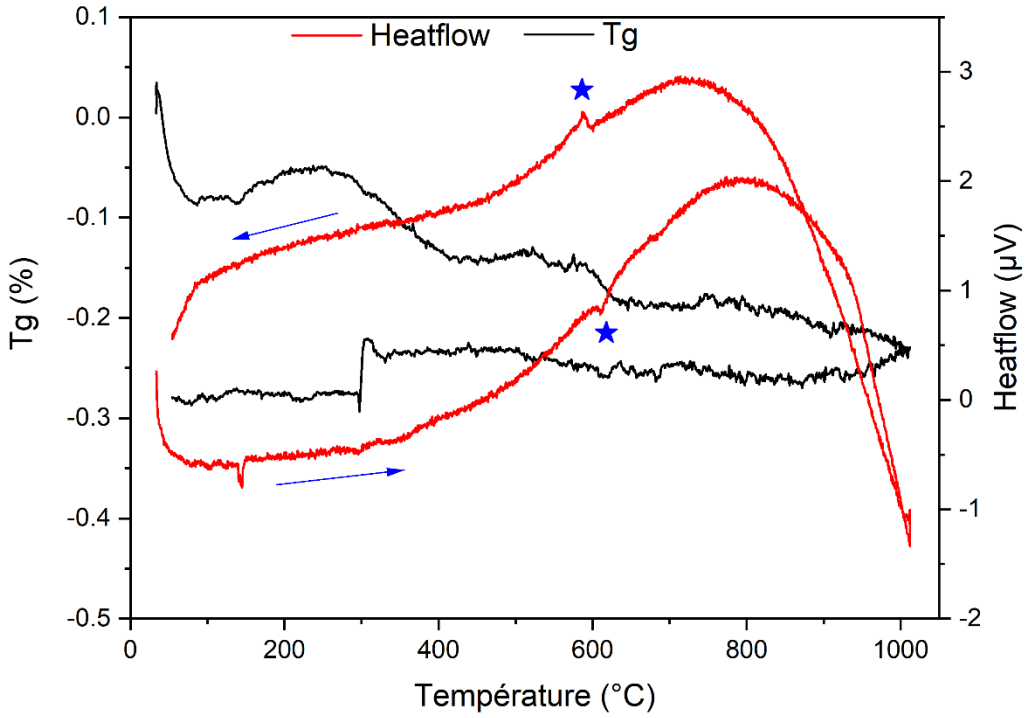

Figure 7: DTA/TG measurement on KBZ powder from room temperature to 1273K. The blue symbol (*) indicates a small reversible peak (885K during heating and 860K during cooling) (color online)

Conclusion

To sum up, the structure of KBZ was studied by room temperature XRD. KBZ presents a prototype cubic perovskite structure (a_p = 4.158Å, Pm3m). Some structural disorder was also evidenced for the K^+/Bi^{3+} pseudo-ion. Since the room temperature space group is centrosymmetric, KBZ presents logically neither piezoelectric nor ferroelectric properties. Unfortunately, KBZ appears difficult to sinter and only low relative densities were obtained (80-90%). However, electrostriction was observed at room temperature, which is a favourable situation to induce ferroelectric/relaxor/piezoelectric properties by appropriate chemical substitution. Because of the mixed occupancy of the A-site by the (K^+/Bi^{3+}) pseudo-ion, KBZ could also exhibit relaxor

properties, similar to the one of PMN. However dielectric measurements could not confirm the existence of such relaxor behaviour. Above room temperature, KBZ remains cubic up to 1273K (1000°C) without any decomposition. Below room temperature, a small reversible thermal anomaly is observed by DSC (250-290K). Further structural study will be necessary in order to check for a possible phase transition associated to this phenomenon. However, the occurrence of electrostriction combined to the limited evolution of the relative permittivity as a function of temperature indicate that this compound may be an interesting material, provided that the sintering of KBZ can be improved.

Acknowledgments

J. Lelievre wants to thanks the “Region Limousin” which granted its thesis scholarship, the “Region Nouvelle Aquitaine” for post-doc funding and the Laboratoire Léon Brillouin, Orsay, France (LLB) for beam time and help in neutron diffraction experiments.

References

[1] A.J. Bell, O. Deubzer, Lead-free piezoelectrics - The environmental and regulatory issues, MRS Bull. 43 (2018) 581–587. https://doi.org/10.1557/mrs.2018.154.

[2] RoHS directive, Directive 2011/65/EU of the European Parliament and of the Council of 8 June 2011 on the restriction of the use of certain hazardous substances in electrical and electronic equipment (RoHS), Official Journal of the European Union. L174 (2011) 88–110.

[3] WEEE directive, Directive 2012/19/EU of the European Parliament and of the Council of 4 July 2012 on waste electrical and electronic equipment (WEEE), Official Journal of the European Union. L197 (2012) 38–71.

[4] W. Liu, X. Ren, Large Piezoelectric Effect in Pb-Free Ceramics, Phys. Rev. Lett. 103 (2009) 257602. https://doi.org/10.1103/PhysRevLett.103.257602.

[5] M.D. Maeder, D. Damjanovic, N. Setter, Lead Free Piezoelectric Materials, J Electroceram. 13 (2004) 385–392. https://doi.org/10.1007/s10832-004-5130-y.

[6] Y. Saito, H. Takao, T. Tani, T. Nonoyama, K. Takatori, T. Homma, T. Nagaya, M. Nakamura, Lead-free piezoceramics, Nature. 432 (2004) 84–87. https://doi.org/10.1038/nature03028.

[7] S. Zhang, R. Xia, T.R. Shrout, Lead-free piezoelectric ceramics vs. PZT?, J. Electroceram. 19 (2007) 251–257. https://doi.org/10.1007/s10832-007-9056-z.

[8] T. Takenaka, H. Nagata, Y. Hiruma, Y. Yoshii, K. Matumoto, Lead-free piezoelectric ceramics based on perovskite structures, J. Electroceram. 19 (2007) 259–265. https://doi.org/10.1007/s10832-007-9035-4.

[9] J. Rödel, W. Jo, K.T.P. Seifert, E.-M. Anton, T. Granzow, D. Damjanovic, Perspective on the Development of Lead-free Piezoceramics, J. Am. Ceram. Soc. 92 (2009) 1153–1177. https://doi.org/10.1111/j.1551-2916.2009.03061.x.

[10] P.K. Panda, Review: environmental friendly lead-free piezoelectric materials, J. Mater. Sci. 44 (2009) 5049–5062. https://doi.org/10.1007/s10853-009-3643-0.

[11] S.O. Leontsev, R.E. Eitel, Progress in engineering high strain lead-free piezoelectric ceramics, Sci. Technol. Adv. Mater. 11 (2010) 044302. https://doi.org/10.1088/1468-6996/11/4/044302.

[12] J. Rödel, K.G. Webber, R. Dittmer, W. Jo, M. Kimura, D. Damjanovic, Transferring lead-free piezoelectric ceramics into application, J. Eur. Ceram. Soc. 35 (2015) 1659–1681. https://doi.org/10.1016/j.jeurceramsoc.2014.12.013.

[13] M.H. Lee, D.J. Kim, J.S. Park, S.W. Kim, T.K. Song, M.-H. Kim, W.-J. Kim, D. Do, I.-K. Jeong, High-Performance Lead-Free Piezoceramics with High Curie Temperatures, Adv. Mater. 27 (2015) 6976–6982. https://doi.org/10.1002/adma.201502424.

[14] P.K. Panda, B. Sahoo, PZT to Lead Free Piezo Ceramics: A Review, Ferroelectrics. 474 (2015) 128–143. https://doi.org/10.1080/00150193.2015.997146.

[15] M. Acosta, N. Novak, V. Rojas, S. Patel, R. Vaish, J. Koruza, G.A. Rossetti, J. Rödel, $BaTiO_3$-based piezoelectrics: Fundamentals, current status, and perspectives, Appl. Phys. Rev. 4 (2017) 041305. https://doi.org/10.1063/1.4990046.

[16] J. Suchanicz, K. Kluczewska, P. Czaja, B. Handke, M. Sokolowski, A. Węgrzyn, G. Stachowski, Influence of sintering conditions on structural, thermal, electric and ferroelectric properties of $Na_{0.5}Bi_{0.5}TiO_3$ ceramics, Phase Transit. 91 (2018) 26–37. https://doi.org/10.1080/01411594.2017.1341982.

[17] Y. Li, W. Chen, Q. Xu, J. Zhou, X. Gu, Piezoelectric and ferroelectric properties of $Na_{0.5}Bi_{0.5}TiO_3$–$K_{0.5}Bi_{0.5}TiO_3$–$BaTiO_3$ piezoelectric ceramics, Mater. Lett. 59 (2005) 1361–1364. https://doi.org/10.1016/j.matlet.2004.12.041.
[18] Q. Xu, S. Chen, W. Chen, S. Wu, J. Zhou, H. Sun, Y. Li, Synthesis and piezoelectric and ferroelectric properties of $(Na_{0.5}Bi_{0.5})_{1-x}Ba_xTiO_3$ ceramics, Mater. Chem. Phys. 90 (2005) 111–115. https://doi.org/10.1016/j.matchemphys.2004.10.018.
[19] G.A. Smolenskii, New ferroelectrics of complex composition, Soviet Physics - Solid State. (1961) 2651–2654.
[20] G.A. Smolenskii, N.N. Krainik, N.P. Khuchua, V.A. Isupov, V.V. Zhdanova, O.M. Mushtare, A.Y. Cherkash, Some ferroelectric and antiferroelectric materials with high Curie points, Izv. Akad. Nauk Ser. Fiz. (1967) 1164–1167.
[21] Y. Yamada, T. Akutsu, H. Asada, K. Nozawa, S. Hachiga, T. Kurosaki, O. Ikagawa, H. Fujiki, K. Hozumi, T. Kawamura, T. Amakawa, K. Hirota, T. Ikeda, Effect of B-Ions Substitution in $[(K_{1/2}Bi_{1/2})$-$(Na_{1/2}Bi_{1/2})](Ti$-$B)O_3$ System with B=Zr, $Fe_{1/2}Nb_{1/2}$, $Zn_{1/3}Nb_{2/3}$ or $Mg_{1/3}Nb_{2/3}$, Jpn. J. Appl. Phys. 34 (1995) 5462. https://doi.org/10.1143/JJAP.34.5462.
[22] Lily, K. Kumari, K.L. Prasad, K.L. Yadav, Dielectric and impedance study of lead-free ceramic: $(Na_{0.5}Bi_{0.5})ZrO_3$, J Mater Sci. 42 (2007) 6252–6259. https://doi.org/10.1007/s10853-006-0824-y.
[23] K. Prasad, Lily, K. Kumari, K.L. Yadav, Hopping type of conduction in $(Na_{0.5}Bi_{0.5})ZrO_3$ ceramic, J. Phys. Chem. Solids. 68 (2007) 1508–1514. https://doi.org/10.1016/j.jpcs.2007.03.023.
[24] P. Jaiban, J. Sukanda, W. Anucha, Densification of $Bi_{0.5}Na_{0.5}ZrO_3$ ceramic using liquid-phase sintering method, Science Asia. (2011) 256–261.
[25] P. Jaiban, A. Rachakom, S. Buntham, S. Jiansirisomboon, A. Watcharapasorn, Fabrication of $Bi_{0.5}Na_{0.5}ZrO_3$ Powder by Mixed Oxide Method, Mater. Sci. Forum. 695 (2011) 49–52. https://doi.org/10.4028/www.scientific.net/MSF.695.49.
[26] P. Jaiban, S. Jiansirisomboon, A. Watcharapasorn, R. Yimnirun, R. Guo, A.S. Bhalla, High- and low-field dielectric responses and ferroelectric properties of $(Bi_{0.5}Na_{0.5})Zr_{1-x}Ti_xO_3$ ceramics, Ceram. Int. 39 (2013) S81–S85. https://doi.org/10.1016/j.ceramint.2012.10.039.
[27] E.T. Wefring, M.I. Morozov, M.-A. Einarsrud, T. Grande, Solid-State Synthesis and Properties of Relaxor (1−x)BKT–xBNZ Ceramics, J. Am. Ceram. Soc. 97 (2014) 2928–2935. https://doi.org/10.1111/jace.13066.
[28] J. Lelievre, M. Josse, P. Marchet, Structure and properties of $(Na_{0.5}Bi_{0.5})ZrO_3$ (NBZ) lead-free perovskite compound, Scripta Mater. 161 (2019) 13–17. https://doi.org/10.1016/j.scriptamat.2018.10.003.
[29] M. Bengagi, F. Morini, M.E. Maaoui, P. Marchet, Structure and electrical properties in the $K_{1/2}Bi_{1/2}TiO_3$–$K_{1/2}Bi_{1/2}ZrO_3$ solid solution (KBT–KBZ), Phys. Status Solidi (a). 209 (2012) 2063–2072. https://doi.org/10.1002/pssa.201127327.
[30] T. Zheng, Y. Zu, J. Wu, Composition dependence of phase structure and electrical properties in lead-free (1-x)$(K_{0.42}Na_{0.585})(Nb_{1-y}Sb_y)O_3$-x$Bi_{0.5}K_{0.5}ZrO_3$ piezoceramics, J. Alloy. Compd. 647 (2015) 927–934. https://doi.org/10.1016/j.jallcom.2015.05.250.
[31] S. Liu, P.E.R. Blanchard, Z. Zhang, B.J. Kennedy, C.D. Ling, Long- and short-range structure studies of KBT-KBZ solid-solutions using synchrotron radiation, Dalton Trans. 44 (2015) 10681–10688. https://doi.org/10.1039/C4DT03866E.
[32] S. Feng, D. Xiao, J. Wu, M. Xiao, J. Zhu, Lead-free (K, Na)NbO_3–$Bi_{0.5}K_{0.5}ZrO_3$–$BaZrO_3$ ternary system: Microstructure and electrical properties, J. Alloy. Compd. 619 (2015) 560–563. https://doi.org/10.1016/j.jallcom.2014.09.032.

[33] T. Yan, S. Ren, X. Ma, F. Han, L. Fang, B. Peng, L. Liu, X. Kuang, B. Elouadi, Dielectric Properties of $(Bi_{0.5}K_{0.5})ZrO_3$ Modified $(K_{0.5}Na_{0.5})NbO_3$ Ceramics as High-Temperature Ceramic Capacitors, J. Electron. Mater. 47 (2018) 7106–7113. https://doi.org/10.1007/s11664-018-6641-7.
[34] G. Hernandez-Cuevas, J.R. Leyva Mendoza, P.E. García-Casillas, C.A. Rodríguez González, J.F. Hernandez-Paz, G. Herrera-Pérez, L. Fuentes-Cobas, S. Díaz de la Torre, O. Raymond-Herrera, H. Camacho-Montes, Effect of the sintering technique on the ferroelectric and d33 piezoelectric coefficients of $Bi_{0.5}(Na_{0.84}K_{0.16})_{0.5}TiO_3$ ceramic, J. Adv. Ceram. 8 (2019) 278–288. https://doi.org/10.1007/s40145-019-0314-8.
[35] PDF 00-057-0823, 00-067-0245 and 04-022-2727, (n.d.).
[36] J. Suchanicz, A. Kania, P. Czaja, A. Budziak, A. Niewiadomski, Structural, thermal, dielectric and ferroelectric properties of $K_{0.5}Bi_{0.5}TiO_3$ ceramics, J. Eur. Ceram. Soc. 38 (2018) 567–574. https://doi.org/10.1016/j.jeurceramsoc.2017.09.036.
[37] L.E. Cross, Relaxor ferroelectrics: An overview, Ferroelectrics. 151 (1994) 305–320. https://doi.org/10.1080/00150199408244755.
[38] V. Petříček, M. Dušek, L. Palatinus, Crystallographic Computing System JANA2006: General features, Z. Kristall. 229 (2014) 345–352. https://doi.org/10.1515/zkri-2014-1737.
[39] R.D. Shannon, C.T. Prewitt, Effective ionic radii in oxides and fluorides, Acta Crystallogr. B25 (1969) 925–946. https://doi.org/10.1107/S0567740869003220.
[40] R.D. Shannon, C.T. Prewitt, Revised values of effective ionic radii, Acta Crystallogr. B26 (1970) 1046–1048. https://doi.org/10.1107/S0567740870003576.
[41] R.D. Shannon, Revised effective ionic radii and systematic studies of interatomic distances in halides and chalcogenides, Acta Crystallogr. A32 (1976) 751–767. https://doi.org/10.1107/S0567739476001551.
[42] A.M. Glazer, The classification of tilted octahedra in perovskites, Acta Crystallogr. B28 (1972) 3384–3392. https://doi.org/10.1107/S0567740872007976.
[43] A.M. Glazer, Simple ways of determining perovskite structures, Acta Crystallogr. A31 (1975) 756–762. https://doi.org/10.1107/S0567739475001635.
[44] C.J. Howard, H.T. Stokes, Group-Theoretical Analysis of Octahedral Tilting in Perovskites, Acta Crystallogr. B54 (1998) 782–789. https://doi.org/10.1107/S0108768198004200.
[45] N. de Mathan, E. Husson, P. Gaucher, A. Morell, Modification of the B-site order of $PbMg_{1/3}Nb_{2/3}O_3$ ceramics by thermal annealing or by La-doping, Mater. Res. Bull. 25 (1990) 427–434. https://doi.org/10.1016/0025-5408(90)90177-4.
[46] P. Bonneau, P. Garnier, G. Calvarin, E. Husson, J.R. Gavarri, A.W. Hewat, A. Morell, X-ray and neutron diffraction studies of the diffuse phase transition in $PbMg_{1/3}Nb_{2/3}O_3$ ceramics, J. Solid State Chem. 91 (1991) 350–361. https://doi.org/10.1016/0022-4596(91)90090-5.
[47] G.O. Jones, P.A. Thomas, Investigation of the structure and phase transitions in the novel A-site substituted distorted perovskite compound $Na_{0.5}Bi_{0.5}TiO_3$, Acta Crystallogr. B58 (2002) 168–178. https://doi.org/10.1107/S0108768101020845.
[48] G.O. Jones, J. Kreisel, P.A. Thomas, A structural study of the $(Na_{1-x}K_x)_{0.5}Bi_{0.5}TiO_3$ perovskite series as a function of substitution (x) and temperature, Powder Diffr. 17 (2002) 301–319. https://doi.org/10.1154/1.1505047.
[49] M. Josse, M. Dubois, M. El-Ghozzi, D. Avignant, Crystal structure of $RbAl_2Tb_4F_{22}$: A second example of mixed-valence fluoroterbate with a random distribution of Tb^{3+} and Tb^{4+} ions, Solid State Sci. 7 (2005) 89–96. https://doi.org/10.1016/j.solidstatesciences.2004.10.025.
[50] T. Ikeda, Fundamentals of piezoelectricity, Oxford University Press, Oxford, 1996.
[51] E. Lattard, M. Lejeune, P. Abelard, Electrostrictive properties of $PbMg_{1/3}Nb_{2/3}O_3$ (PMN) bulk ceramics, J. Phys. III. 4 (1994) 1165–1187. https://doi.org/10.1051/jp3:1994193.

[52] D. Taylor, Thermal Expansion Data VIII. Complex oxides, ABO_3, the perovskites., Trans. & J. British Ceram. Soc. 84 (1985) 181–188.

Figure

Click here to access/download;Figure;Fig 1.tiff

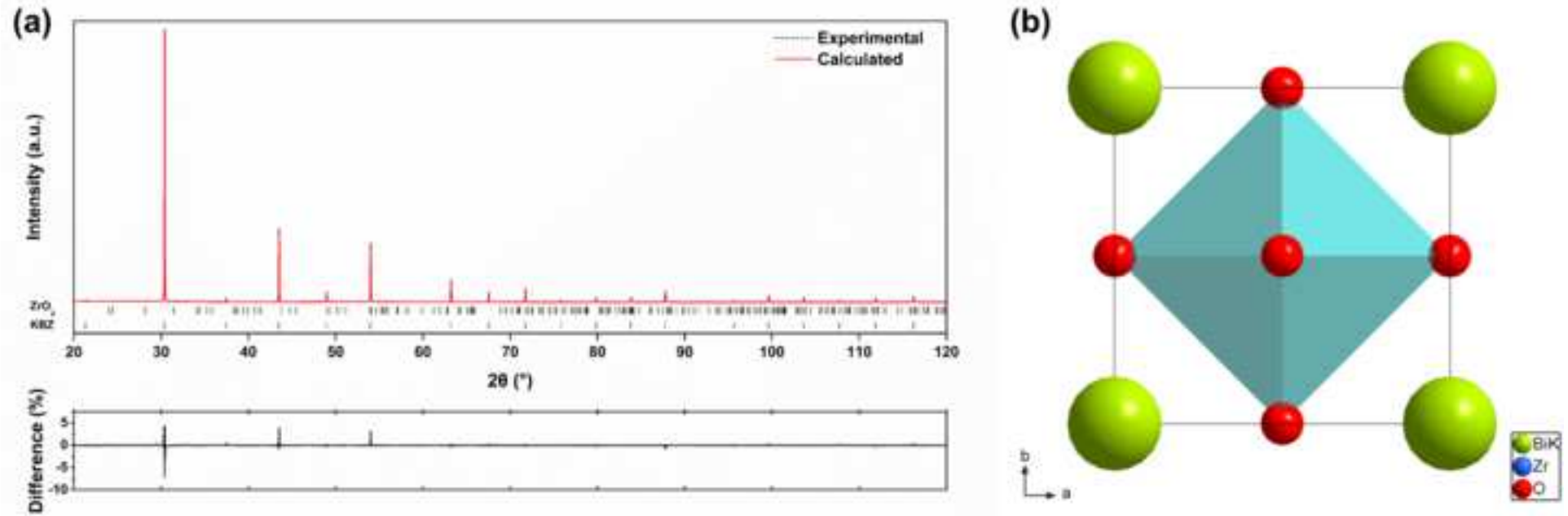

Figure

Click here to access/download;Figure;Fig 2.tiff

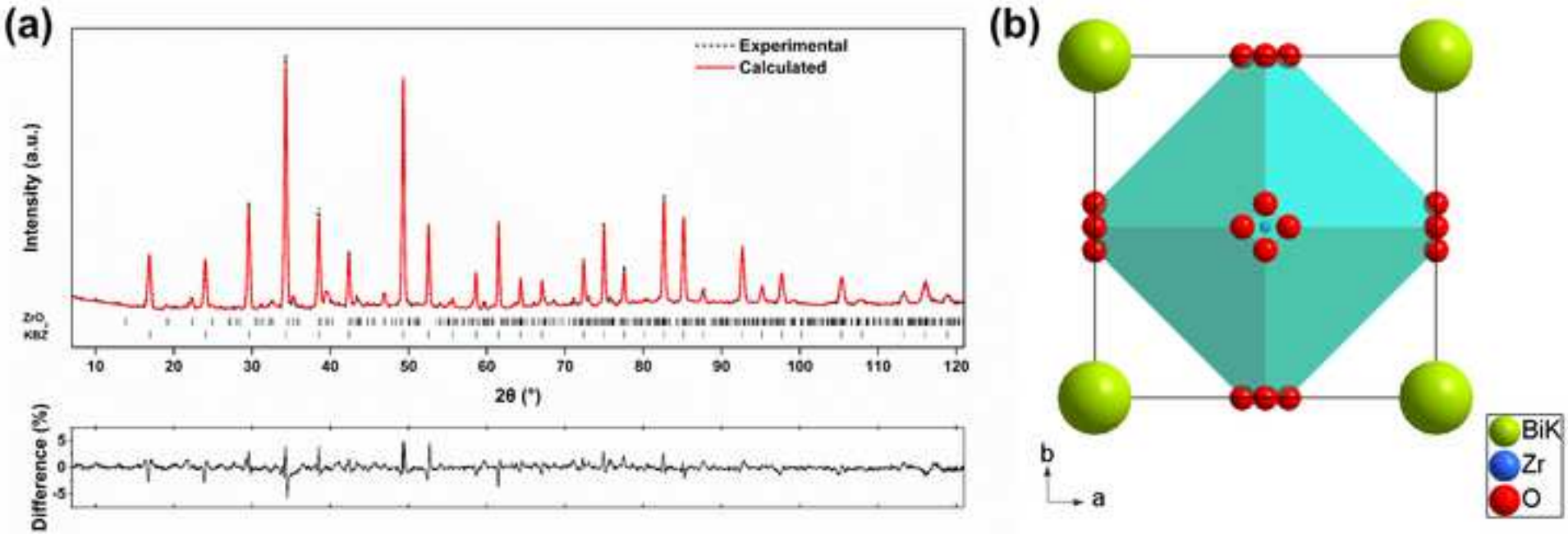

Figure

Click here to access/download;Figure;Fig 3.tif

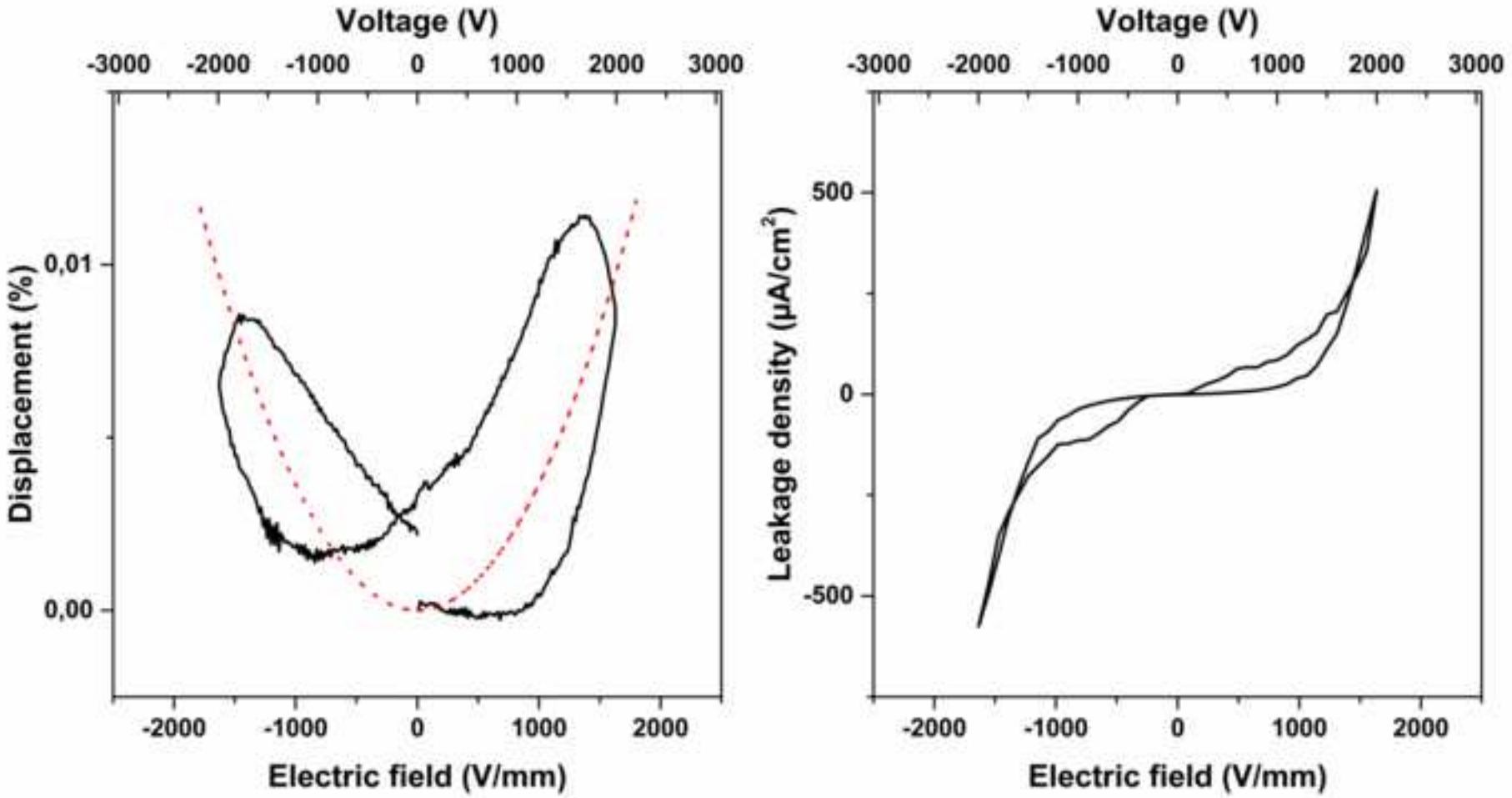

Figure

Click here to access/download;Figure;Fig 4.tif

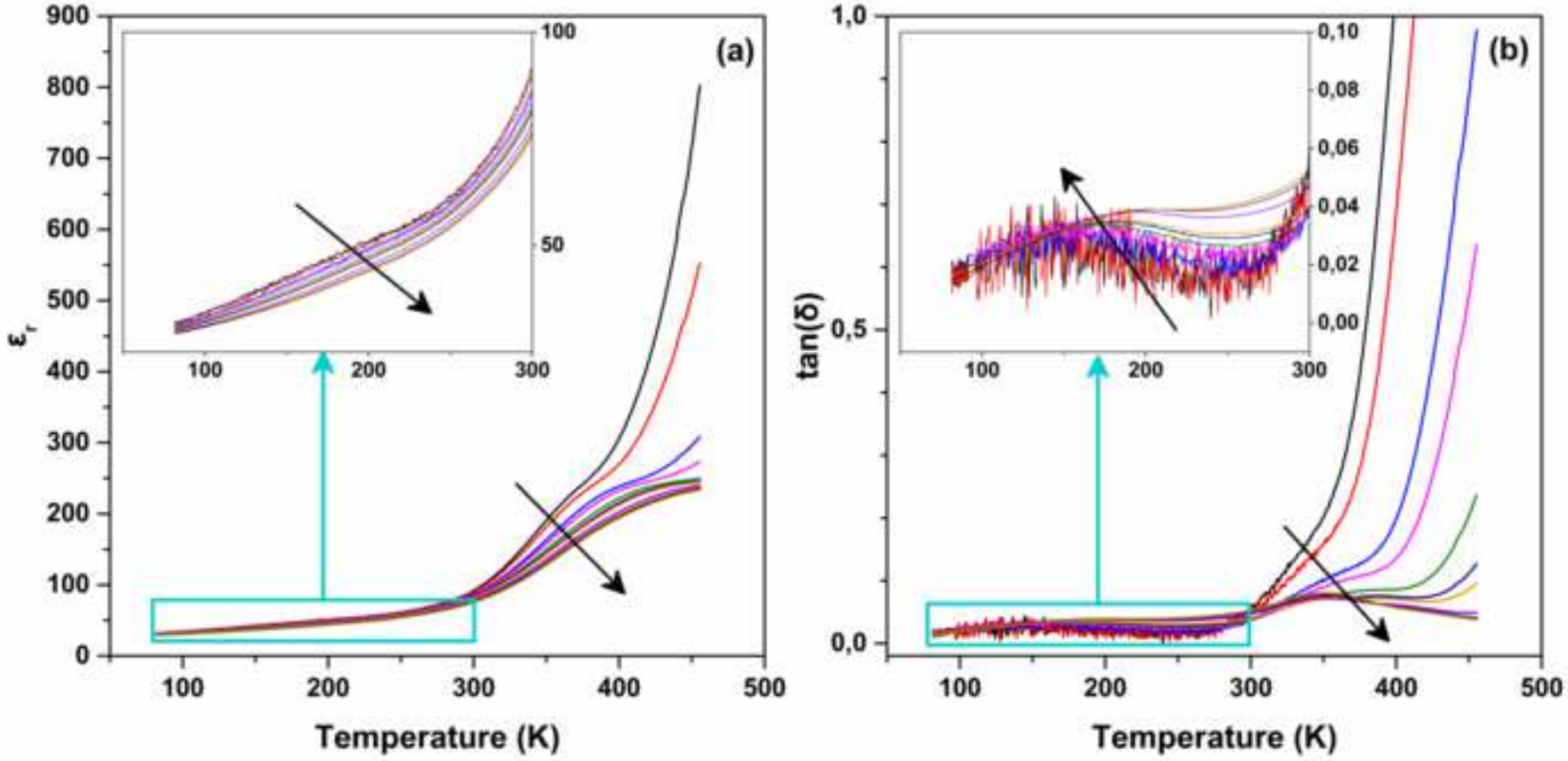

Figure

Click here to access/download;Figure;Fig 5.tif

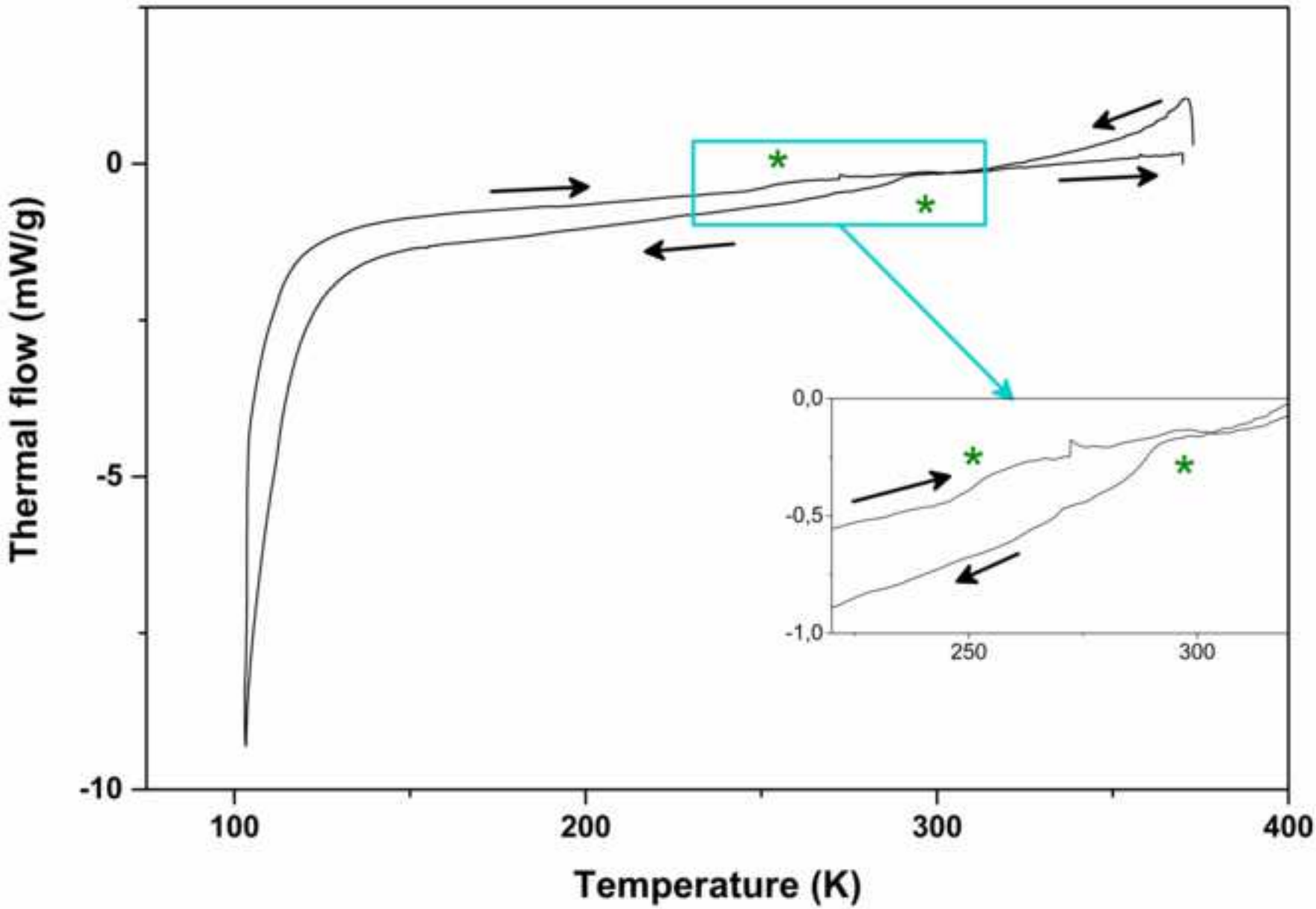

Figure

Click here to access/download;Figure;Fig 6.tif

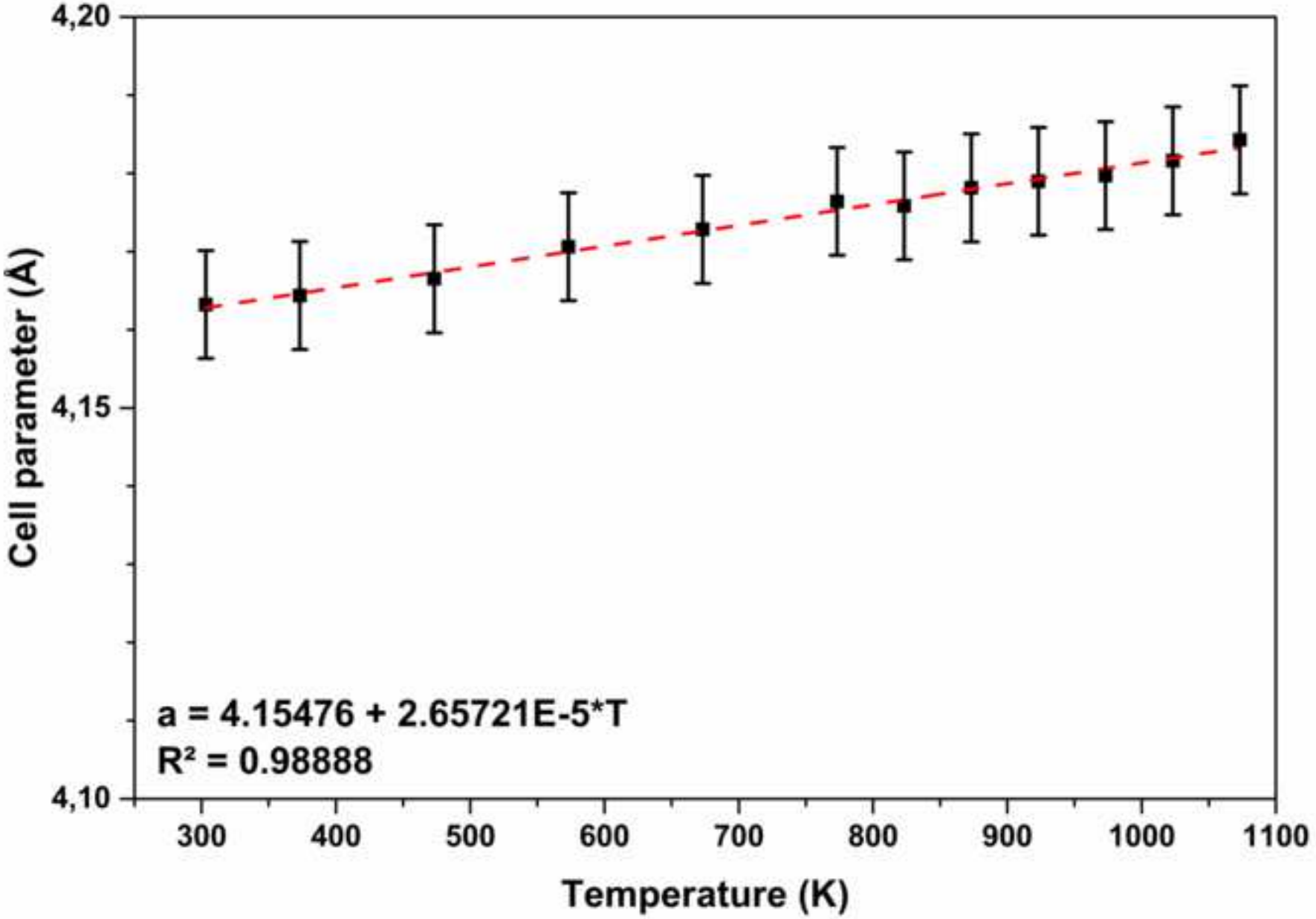

Figure

Click here to access/download;Figure;fig 7.tif